Ultrasonic Evaluation of Microcracks in Composites

V. DAYAL*, V. IYER** and V. K. KINRA**

*Mechanical Engineering Department, N. C. A & T State University, Greensboro, N. C. 27411, USA

**Aerospace Engineering Department, Texas A & M University, College Station, Texas 77843, USA

ABSTRACT

Acoustic parameters, namely, wavespeed and attenuation are measured precisely. The variations in these properties due to the presence of microcracks are used to characterize damage in composites. Two methods have been used to measure the acoustic parameters, one utilizing P-wave propagating in through-the-thickness direction and the other utilizing leaky lamb waves propagating in in-plane direction. These results have been compared with those reported in literature.

KEYWORDS

Microcracks; Composites; Leaky lamb waves; Wavespeed; Attenuation; P-wave, Through-the-thickness; In-plane.

INTRODUCTION

Microcracks in composites can develop due to mechanical, thermal or humidity loading. These cracks develop in the matrix material. A crack acts as stress raiser and the fibers are able to transfer the stresses to other locations in the composite component. As a result the next crack develops at some other location where the stresses exceed the critical limits. Finally, the entire structure may develop these microcracks. These cracks do not endanger the integrity of the structure but reduce the load bearing capacity of the structure. Also, the damping characteristics of the material are changed. These cracks are small and so widely spread that it is rather difficult to identify them individually. Theories are being developed to study the effect of the cracks on the overall behavior of the structure but they are far from being of practical value.

It is well known that the stiffness of a material can be related to the wavespeed of the sound wave traveling through it by the relation, $c^2 = E/\rho$, where c is the wavespeed of sound in the material, E

is an appropriate stiffness and ρ is the density of the material. The attenuation of sound in the medium is the damping property of the material. Hence if the acoustic parameters, namely, wavespeed and attenuation of the sound in a medium can be accurately measured then the stiffness and damping can be calculated. The aim of this work is a precise measurement of the acoustic parameters so that the variations in the properties due to the microcracks can be detected. The computerized techniques developed by us are capable of measuring the changes in acoustic parameters even for a single crack. But keeping in view the practical aspects of the work, we have tested specimens with multiple cracks. Moreover, when there are multiple cracks the damage state can be treated from the continuum mechanics point of view.

Composite specimen are generally made in the form of thin sheets. The ultrasonic waves can be propagated in these structures in two different directions: first, normal to the sheet and second, in the plane of the sheet. The wave speeds in these two directions will depend on the stiffness in the respective directions. We have propagated the ultrasonic waves both in the direction normal to the plate and in the plane of the plate. In the plane of the plate the waves were restricted to only the x-direction of the laminate. Presented here are the results from both type of tests. The goal is to demonstrate that ultrasonic NDE is a very powerful tool for the measurement of the changes in the basic mechanical properties.

THEORY

For a detailed analysis of the case when the waves travel normal to the specimen, the interested reader is referred to (Kinra et al., 1987). The following relations are presented for completeness.

Fig. 1 shows the various transmitted and reflected pulses when an incident wave impinges on a plate specimen. If the pulses can be separated in the time domain and the reflected pulses are captured then the following equation is obtained,

$$G^*/F^* = 1 - T_{12}T_{21}\exp(-i2kh) \qquad (1)$$

where G^* = the FFT of two pulses

F^* = the FFT of the first pulse

T_{ij} = transmission coefficient from medium i to j

R_{ij} = reflection coefficient when wave traveling in medium i reflects from i/j interface.

h = the sample thickness

$k = k_1 + ik_2$ is the complex wave number

$k_1 = \omega/c$ is the wavenumber

ω = the circular frequency

c = the wavespeed

k_2 = the attenuation

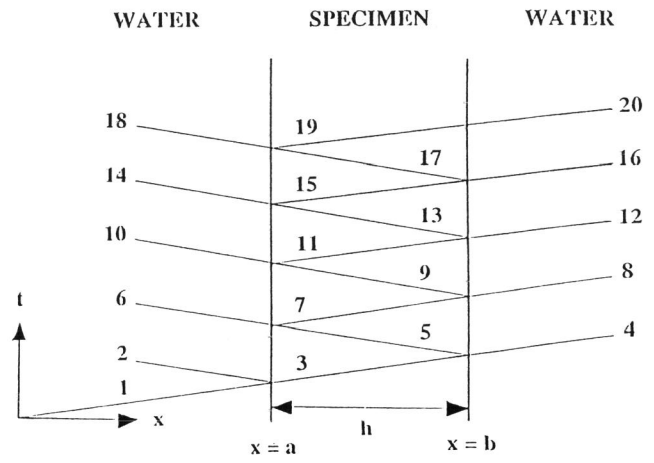

Fig. 1. Various reflections and transmissions from a plate immersed in water.

Substituting $k = k_1 + ik_2$ into eq. (1) and comparing the real and imaginary parts on the two sides we get,

$$c = 4\pi h/(-\phi/f) \text{ and } k_2 = \ln(M)/2h$$

where ϕ = phase of (G^*/F^*-1),

and, $M = |G^* F^*-1/(T_{12}T_{21})|$ in water immersion,

If the pulses cannot be separated then for the reflected field,

$$\exp(-i2kh) = [\beta/(1+\beta)]/R_{21}^2$$

where $\beta = R_{12}R_{21}[G^*/F^* -1]/(T_{12}T_{21})$

here G^* is the FFT of the entire reflected field and F^* is the FFT of a reference signal.

If the transmitted pulses are captured and individual pulses can be separated in time domain then,

$$G^*/F^* = T_{12}T_{21}\exp[-i(kh - k_o h)] \qquad (2)$$

where k_o is the wavenumber in water. As in the reflection case we obtain,

$$c = 2\pi h/(-\phi/f) \text{ and } k_2 = \ln(M)/h \text{ where } M = |G^*/F^*/T_{12}T_{21}| \qquad (3)$$

For the transmitted field, if the individual pulses cannot be separated,

$$G^*/F^* = T_{12}T_{21}\exp[-ih(k-k_o)]/[1-R_{21}^2\exp(-i2kh)] \qquad (4)$$

here F* is the FFT of the signal at receiver when there is no sample between the two transducers and G* is the FFT of the total transmitted signal after the sample is introduced in the wave path.

For the Lamb wave tests we have used the fundamental symmetric mode of wave propagation. The reason behind this choice is that in this mode the wave travels with a plane wavefront. The relation between the material properties and wavespeed in the fundamental symmetric mode (Dayal 1987), is

$$C_L^2 = E_1/[\rho(1-\nu_1^2\nu_{21})] \tag{5}$$

where C_L is the Lamb wavespeed,

E_1 is the in-plane modulus,

ν_{12} is the major Poisson's ratio, and
ν_{21} is the minor Poisson's ratio.

For the composites used by us $\nu_{12} = 0.28$ and $\nu_{21} = 0.018$. Thus, $\nu_{12}\nu_{21} << 1$ and, to a first approximation,

$$C_L^2 = E_1/\rho \tag{6}$$

The relation between the angle of incidence of the wave on the plate, θ_i, and the wavespeed (C_L) of the Lamb wave is governed by the Snell's Law;

$$\sin(\theta_i)/V_w = \sin(\pi/2)/C_L \tag{7}$$

where V_w is the wavespeed in water.

EXPERIMENTAL SETUP

The block diagram of the experimental setup is shown in Fig. 2. The specimen, the transmitter and the receiver are immersed in the water bath. The specimen is mounted on a turn table and can be rotated about a vertical axis in steps of 0.1 degrees. This rotation is required to set the specimen for the through-the-thickness and Lamb wave measurements. The transducers are mounted on precision traveling mechanisms. In the through-the-thickness measurements the specimen is normal to the incident wave and the two transducers are in the same line.

The pulse generator triggers the signal generator which produces a single cycle of sinusoidal wave for through-the-thickness measurements and a tone burst for the Lamb wave measurements. This signal is amplified by the power amplifier and the signal is fed into the wide band transmitting transducer. The wave launched in the water travels through the specimen and is sensed by the receiving transducer. The signal from the receiver is amplified by the signal amplifier and fed into a Digitizing Oscilloscope (Data 6000 by Data Precision). The analog signal is digitized and stored in the oscilloscope. The built-in signal is digitized and stored in the oscilloscope. The built-in signal

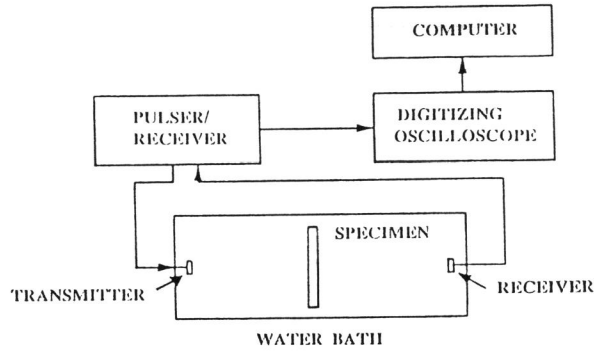

Fig 2. Schematic of the experimental set-up.

processor of this oscilloscope provides the computer with the information needed for further signal processing. In the case of through-the-thickness tests this information is in the form of Fourier Transform of the signals and in the Lamb wave tests it is the amplitude and location of a characteristic point of the toneburst signal e.g. a maximum of a sine wave. For the through-the-thickness case the wavespeed and attenuation are calculated by using the appropriate equation from the theory section. In the Lamb wave test the signal amplitude at different angles of incidence is recorded. Critical Lamb angle is identified by the peak in the received signal.

All the specimens for which the results are presented here are made of AS4/3502 Graphite/Epoxy laminates. The specimens are 11"x1" coupons.

All loading to induce damage in the specimen was performed on INSTRON Model 1125 equipped with a 20,000 lb. load cell. The tests used was 0.05 in./min. A record of the induced damage was kept by the edge replication technique.

RESULTS AND DISCUSSIONS

First, we present some results from the application of the technique where separation of pulses was possible. The variation of attenuation as the load is increased to induce the transverse cracks is shown in Fig. 3 for the specimen of $[0_6/90_4/0_2]$ layup. It is observed that for all damage states the attenuation decreased with an increase in the frequency. The maximum variation is attenuation is observed at a frequency of 2.25 MHz. This figure shows a very dramatic increase in the attenuation as the damage is induced in the specimen. The variation of attenuation, at three locations on the specimen, as the total crack length in the field of observation increases, is shown in Fig. 4. In the early stages of damage when there are a few cracks, some scatter in the attenuation is observed. As more cracks are generated and the continuum damage state is achieved, the attenuation variation becomes steady. The reason is that when there are a few cracks then their location, in the field of the transducer, is critical. A crack in the center of the transducer field will scatter the waves much more than the

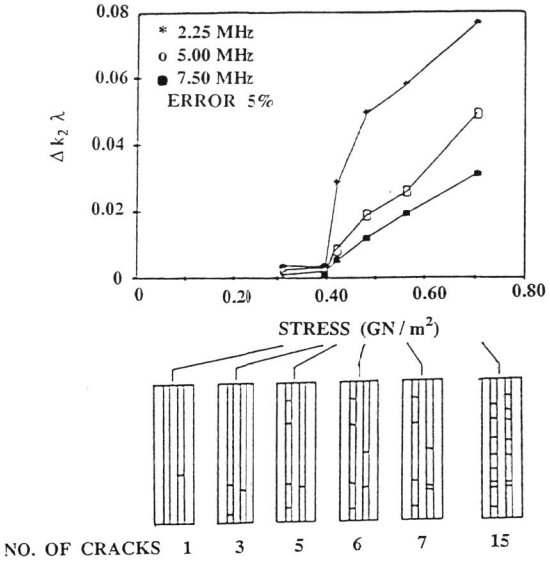

Fig. 3. Attenuation increases dramatically with transverse cracks in Gr/Ep, $[0_6 90_4 0_2]_s$ laminate at all three frequencies tested. Extent of damage is shown in the edge replication sketches.

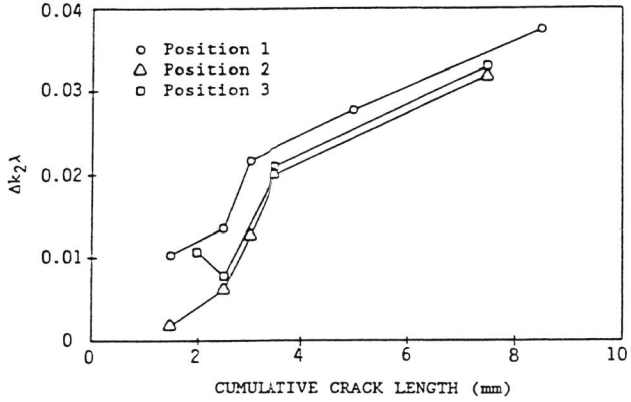

Fig. 4. Attenuation vs. crack length for the laminate in Fig. 3 at 7.5 MHz at three locations on the specimen.

crack at the edge of the field. But when there are a number of cracks then their effect is averaged out and a fairly uniform response is obtained. This shows that such curves can be drawn and will be useful as master curves to quantify the damage. The wavespeeds in the samples were also measured during these tests and it was observed that there was practically no change in the wavespeeds.

The Lamb wave experiment performed on a plate is as follows. The plate is mounted in the rotating specimen-holder and the transducers are set such that they are not directly facing each other. The transmitter is excited with a sinusoidal wavetrain of about 20 cycles at the frequency of interest. The waves sensed at the receiver are recorded and the voltage and time at a particular peak of the signal (about tenth) are measured. The angle of the specimen is changed. Since the length of the specimen between the transducers is increased due to the rotation, the transducers are moved such that exactly the same length of the specimen is under test throughout. At the angle of incidence when the Lamb wave can be sustained in the specimen a large signal is received and is shown as amplitude peak in the signal. These angles are converted to wavespeed via eq. (7). The measurement of attenuation is made as follows. The specimen angle is fixed at the Lamb angle of interest with the transducers suitably placed. Next, the received is moved away by 0.5 inch in steps of 0.05 inch and the amplitude at a particular peak is recorded. An exponential decay curve is fitted through these points and by a least-square-error, the attenuation coefficient is obtained.

The first specimen tested to study the effect of transverse cracks on the Lamb wavespeed and attenuation is $[0/90_3]_s$ laminate. The tests are conducted at a frequency of 0.5 MHz with f.d=0.275 MHz-mm. The reduction in the normalized stiffness as a function of number of cracks per inch as damage progresses is shown in Fig. 5. The normalized stiffness is defined as E/E_o where E_o is the stiffness of the undamaged laminate and E is the stiffness of the damaged laminate.

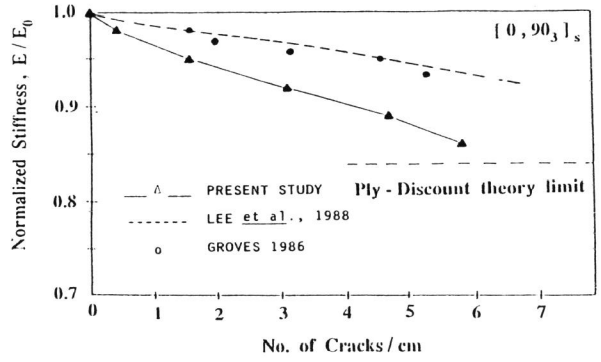

Fig. 5. Reduction in stiffness in $[0/90_3]_s$ laminate, f=0.5 MHz, d=0.55 mm.

The second set of tests was performed on a $[0/90_4]_s$ laminate. The test is performed at 0.5 MHz with f.d=0.355 MHz-mm. The reduction in stiffness for this laminate is shown in Fig. 6. Also shown in the figure is the damage state and the position of the transmitter (TR) and receiver (R). Observe that in going from damage state 3 to state 4, though there was a substantial increase in the total number of cracks in the specimen, the number of cracks in the region interrogated by the transducer did not increase. As a consequence no change in the stiffness of the specimen was recorded. This is very reassuring for it demonstrates that our measurement reflects local changes in the stiffness. For this specimen, stiffness reduced by about 30% as compared to the virgin state. In comparison to the reduction for the $[0/90_3]_s$ laminate it is observed that the stiffness reduction for this laminate is larger. The reason for this is that the net contribution of the eight-90 degree plies to the overall stiffness is more than the contribution of six-90 degree plies to the overall stiffness is more than the contribution of six-90 degree plies and hence failure of plies in the $[0/90_4]_s$ laminates results in a higher reduction in relative stiffness.

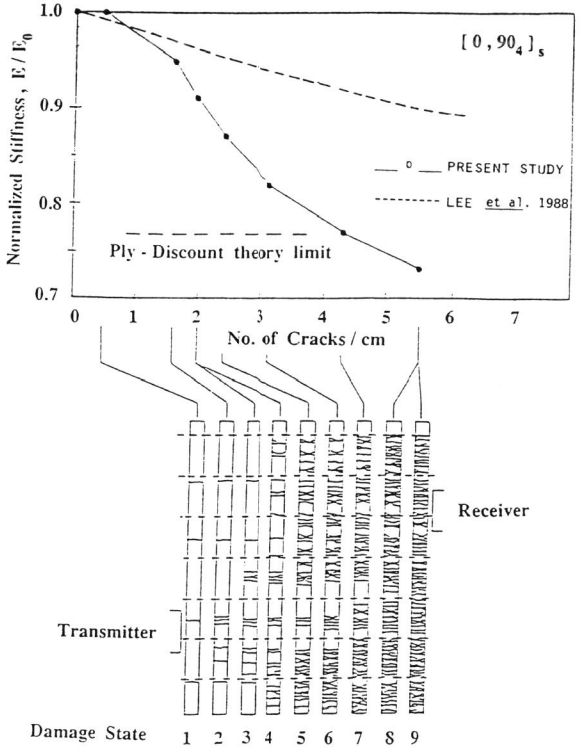

Fig. 6. Reduction in stiffness as transverse cracks increase in a $[0/90_4]_s$ laminate, f=0.5 MHz, d=0.71 mm. Line sketch shows damage state.

The next set of tests was performed on a $[0_2/90_2/0]_s$ laminate. The reduction in stiffness as transverse cracks are introduced is shown in Fig. 7. Observe a smaller reduction in stiffness. Even though this laminate has four-90 degree plies, they are divided into groups of two, and also, the total number of 0 degree plies in this laminate is increased three times. Thus the total contribution of the 90 degree plies to the overall stiffness is very low and hence their failure results in less reduction in stiffness.

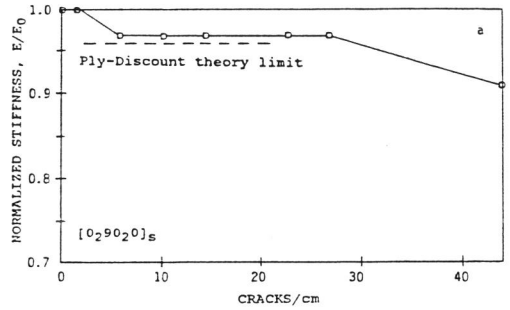

Fig. 7. Reduction in stiffness in $[0_2/90_2/0]_s$ laminate, f=0.5 MHz, d=0.71 mm.

The attenuation increase in the three laminates tested are combined together and shown in Fig. 8. Shown also in the figure are the k_1a values for the three laminates. The purpose of this presentation is to demonstrate the effect of the normalized scattering cross-section of the cracks on the attenuation. In $[0_2/90_2/0]_s$ laminate $k_1a=0.06$, as is well known this is the so-called Rayleigh scattering regime; thus the scattering cross-section of the cracks is very small. For $[0/90_3]_s$ $k_1a=0.26$ and the cracks are able to scatter the waves to a considerable extent. For the $[0/90_4]_s$ laminate $k_1a=0.45$ and the observed increase in attenuation is very high.

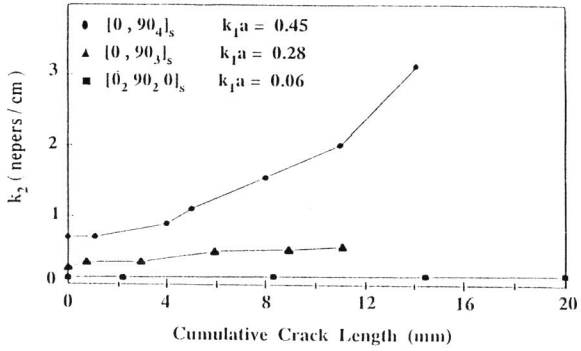

Fig. 8. Relative study of the increase in attenuation for the three laminates tested.

In Figs. 5 and 6 the analytical results of (Lee et al., 1987) based on an internal state variable model are presented. Measurements of static stiffness by (Groves 1988) are also shown in Fig. 5. Clearly there is a significant difference between the ultrasonic measurement and the static measurement. The reason for this systematic differences are not clear at the moment; these differences are being examined and will be the subject of future communication.

CONCLUSIONS

The use of two techniques for ultrasonic nondestructive evaluation of damage (transverse cracking) in laminated composites has been demonstrated. In the first, a longitudinal wave is propagated in the thickness direction. Here the crack-wave interaction is weak. As expected the wavespeed does not change measurably while the attenuation increases with transverse cracking. In the second technique, Lamb waves are propagated along the length of the specimen. Here, the crack-wave interaction is stronger: both the wavespeed and the attenuation change appreciably with damage. The Lamb wave method, therefore, is a much more effective method for the detection of transverse cracks.

ACKNOWLEDGEMENT

This research is supported by the Air Force Office of Scientific Research Contract No. F49620-83-C-0067.

REFERENCES

1. Dayal, V. (1987). Ultrasonic Non-Destructive Evaluation of Fiber-Reinforced Composites, Ph.D. Dissertation, Texas A&M University, College Station, Texas 77843.

2. Groves, S.E. (1986). A Study of Damage Mechanics in Continuous Fiber Composite Laminates with Matrix Cracking and Interply Delaminations, Ph.D. Dissertation, Texas A&M University, College Station, Texas 77843.

3. Kinra, V.K. and Dayal, V. (1987). A New Technique for Ultrasonic NDE of Thin Specimens, to appear in Experimental Mechanics.

4. Lee, J.W., Allen, D.H. and Harris, C.E. (1988). Internal State Variable Approach for Predicting Stiffness Reductions in Fibrous Laminated Composites with Matrix Cracks, Mechanics and Materials Center, Texas A&M University, College Station, Texas 77843.